

京都大学

鍋谷彰 業績リスト

発表者名	論文タイトル名	発表誌名	巻号	ページ	出版年
Nabetani, A. and Ishikawa, F.	Alternative lengthening of telomeres pathway: Recombination-mediated telomere maintenance mechanism in human cells	J. Biochem	149(1)	5-14	2011

Identification of a novel fusion, SQSTM1-ALK, in ALK-positive large B-cell lymphoma

Kengo Takeuchi,¹ Manabu Soda,² Yuki Togashi,¹ Yasunori Ota,³ Yasunobu Sekiguchi,⁴ Satoko Hatano,¹ Reimi Asaka,¹ Masaaki Noguchi,⁴ Hiroyuki Mano^{2,5}

¹Pathology Project for Molecular Targets, Cancer Institute, Japanese Foundation for Cancer Research, Tokyo; ²Division of Functional Genomics, Jichi Medical University, Tochigi; ³Department of Pathology, Toranomon Hospital, Tokyo; ⁴Department of Hematology, Urayasu Hospital, Juntendo University, Chiba; ⁵CREST, Japan Science and Technology Agency, Saitama 332-0012, Japan

ABSTRACT

ALK-positive large B-cell lymphoma is a rare subtype of lymphoma, and most cases follow an aggressive clinical course with a poor prognosis. We examined an ALK-positive large B-cell lymphoma case showing an anti-ALK immunohistochemistry pattern distinct from those of 2 known ALK fusions, CLTC-ALK and NPM-ALK, for the presence of a novel ALK fusion; this led to the identification of SQSTM1-ALK. SQSTM1 is an ubiquitin binding protein that is associated with oxidative stress, cell signaling, and autophagy. We showed transforming activities of SQSTM1-ALK with a focus formation assay and an *in vivo* tumorigenicity assay using 3T3 fibroblasts infected with a recombinant retrovirus encoding SQSTM1-ALK. ALK-inhibitor therapies are promising for treating ALK-positive large B-cell

lymphoma, especially for refractory cases. SQSTM1-ALK may be a rare fusion, but our data provide novel biological insights and serve as a key for the accurate diagnosis of this rare lymphoma.

Key words: ALK-positive, large B-cell lymphoma, fusion.

Citation: Takeuchi K, Soda M, Togashi Y, Ota Y, Sekiguchi Y, Hatano S, Asaka R, Noguchi M, Mano H. Identification of a novel fusion, SQSTM1-ALK, in ALK-positive large B-cell lymphoma. *Haematologica* 2011;96(03):000-000.
doi:10.3324/haematol.2010.033514

©2011 Ferrata Storti Foundation. This is an open-access paper.

Introduction

Anaplastic lymphoma kinase-positive large B-cell lymphoma (ALK+LBCL) is a rare subtype of lymphoma that was first described in 1997.¹ Approximately 50 cases have been reported to date,² with most cases (60%) following an aggressive clinical course.³ In well-characterized cases, 3 genes have been reported as a fusion partner of ALK: *clathrin* (CLTC-ALK),^{4,6} *nucleophosmin* (NPM-ALK),^{7,8} and *SEC31A* (SEC31A-ALK).⁹ In this paper, we report a case of ALK+LBCL that harbored a novel ALK fusion partner, sequestosome1 (SQSTM1).

Design and Methods

Materials

Biopsied specimens were fixed in 20% neutralized formalin and embedded in paraffin for conventional histopathological examination. We extracted DNA and total RNA from the snap-frozen specimens and subsequently purified the samples. Written informed consent was obtained from the patient. The study was approved by the Institutional Review Board of the Japanese Foundation for Cancer Research.

Immunohistochemistry

Formalin-fixed, paraffin-embedded tissue was used. For antigen

retrieval, we heated the slides for 40 min at 97°C in Target Retrieval Solution (pH 9.0; Dako), and subsequently detected the immune complexes with a dextran polymer reagent (EnVision+DAB system, Dako) and an AutoStainer instrument (Dako).

Isolation of ALK fusion cDNA

To obtain cDNA fragments corresponding to novel ALK fusion genes, we used an inverse reverse transcription-polymerase chain reaction (RT-PCR) method slightly modified from one previously reported.¹⁰ Double-stranded cDNA was synthesized from 2 µg of total RNA with 1 pM of the primer ALKREvex22-23 (5'-TGGTTGAATTTGCTGATGATC-3') and a cDNA Synthesis System (Roche), and was self-ligated by incubation overnight with T4 DNA ligase (TaKaRa Bio). We subjected the resulting circular cDNA to PCR (35 cycles of 94°C for 15 sec, 62°C for 30 sec, and 72°C for 1 min) with primers ALKREV3T (5'-CTGATGGAGGAGGTCTTGCC-3') and ALKFWDex20-21 (5'-ATTCGGGGTCTGGCCAT-3') in a final volume of 20 µL. We subjected 1 µL of the 1:100 diluted reaction products to a second PCR step (the same settings as above), with primers ALKREV4T (5'-GGTTGTAGTCGGTCATGATGGTC-3') and ALKFWDex21-22 (5'-AGTGGCTGTGAAGACCGCTGC-3') in a final volume of 20 µL. The resulting products were purified by gel extraction and directly sequenced in both directions with primers ALKFWDex20-21 and ALKREV4T.

The fusion point of SQSTM1-ALK cDNA was amplified by RT-PCR with primers SQSTM1 565F (5'-AAACACGGA-

Acknowledgments: we thank Drs. Masaru Hosone, Yuichi Sugisaki, Koji Izutsu, Shuji Momose, and Jun-ichi Tamaru for their advice. The nucleotide sequences of the cDNAs for SQSTM1-ALK have been deposited in the DDBJ/EMBL/GenBank databases under the accession number, AB583922. Manuscript received on xxxxxxx. Revised version arrived on xxxxxxxxxxxxxxxxx. Manuscript accepted on xxxxxxxxx.

Correspondence: Kengo Takeuchi, M.D., Ph.D. Pathology Project for Molecular Targets, Cancer Institute, Japanese Foundation for Cancer Research. 3-8-31 Ariake, Koto, Tokyo 135-8550, Japan. E-mail: kentakeuchi-ty@umin.net; Tel.: international +81-3-3520-0111; Fax: international +81-3-3570-0558.

CACTTCGGGT-3') and ALK3078RR (5'-ATCCAGTTCGTCCT-GTTCAGAGC-3').

Full-length *SQSTM1-ALK* cDNA was obtained from the specimen by RT-PCR with primers *SQSTM1*v1-F90 (5'-CTCGCTATGCGCTCGCTCACCCTGAA-3') and KA-W-cDNA-out-AS (5'-CCACGGTCTTAGGGATCCCAAGG-3').

Fluorescence in situ hybridization (FISH)

We performed FISH analysis of the gene fusion for unstained slides (4 µm thick) with bacterial artificial chromosome (BAC) clone-derived DNA probes for *ALK* (RP11-984I21, RP11-62B19) and *SQSTM1* (RP11-55M16).

Transformation assay for ALK fusion protein

We analyzed the transforming activity of *SQSTM1-ALK* as described previously.¹¹⁻¹³ Briefly, cDNA for *SQSTM1-ALK* was inserted into the retroviral expression plasmid pMXS.¹⁴ The resulting plasmid and similar pMXS-based expression plasmids for EML4-*ALK* variant 1 or NPM-*ALK* were used to generate recombinant ecotropic retroviruses, which were then used to infect mouse 3T3 fibroblasts. We evaluated formation of transformed foci after culturing the cells for 14 days. We subcutaneously injected the same set of 3T3 cells into nu/nu mice and examined tumor formation after 20 days.

PCR for IGH gene rearrangement

Genomic PCR was used for amplification of the rearranged *IGH* gene using the primers FR2A 5'-TGG(A/G)TCCG(A/C)CAG

(C/G)C(C/T)(C/T)CNGG-3' and LJH 5'-ACCTGAGGAGACG-GTGACC-3'. Several clones were sequenced after subcloning the PCR product into pGEM-T-Easy Vector (Promega).

Results and Discussion

Case presentation

A 67-year old man was admitted with a tumor in the left side of his neck. A systemic workup revealed swelling of cervical, mediastinal, and hilar lymph nodes. Blood counts were within normal ranges. Lactose dehydrogenase was slightly elevated (223 IU/L) in peripheral blood with high IgG (2,425 mg/dL), normal IgA (157 mg/dL) and low IgM (32 mg/dL) levels.

Histopathological examination of the biopsied specimen from the cervical lymph node showed a diffuse infiltrate of tumor cells with a round, vesicular nucleus containing a centrally located large nucleolus. The cytoplasm was abundant (Figure 1A). These features may be consistent with immunoblasts or plasmablasts, but the size of tumor cells was large compared with typical immunoblasts and plasmablasts. Immunophenotypically, the tumor cells were negative for CD3, CD4, CD5, CD10, CD20, CD57, CD79a, and most cytokeratins (CK5/6, CK8, CK19, CK20); focally positive for CD30 and cytokeratins (AE1/AE3, CAM5.2, CK7, CK18) (Figure 1B); weakly positive for PAX5; and positive for CD138 (Figure

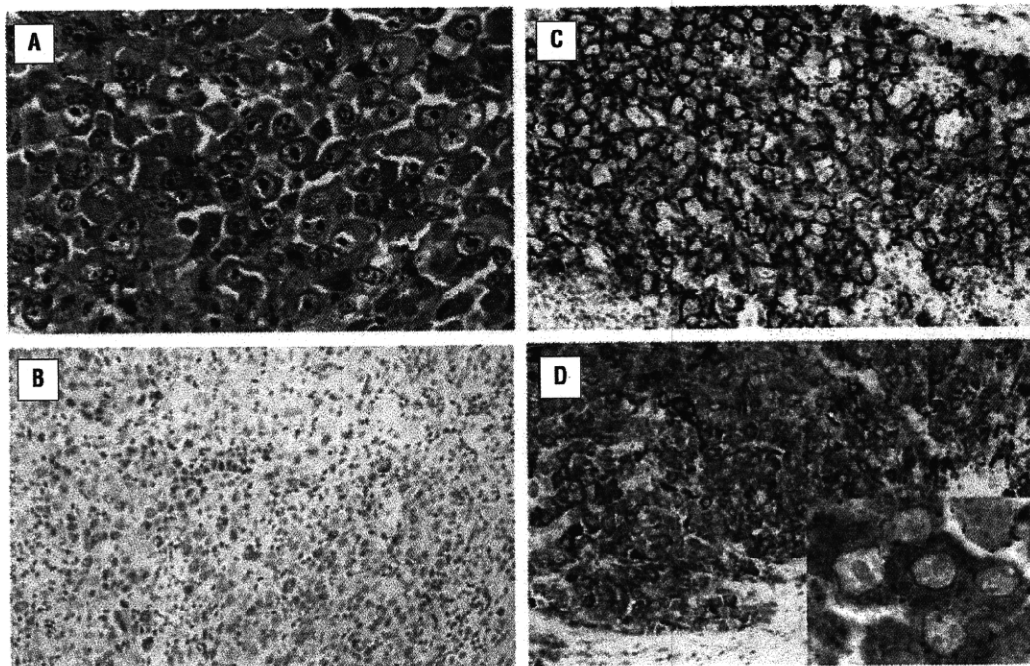


Figure 1. Histopathology of *SQSTM1-ALK*-positive large B-cell lymphoma. (A) The pattern of tumor infiltration was diffuse. The lymphoma cells were large with abundant cytoplasm and had round, vesicular nuclei, each containing a centrally located large nucleolus. These features may be consistent with immunoblasts or plasmablasts, but the size of tumor cells was extremely large compared with these typical cell types (40× objective). (B) Some lymphoma cells expressed cytokeratin (AE1/AE3) (20× objective). (C) Syndecan1/CD138 was strongly expressed (20× objective). (D) In anti-*ALK* immunohistochemistry, a diffuse cytoplasmic staining pattern with ill-demarcated spots was clearly shown (20× objective).

1C), EMA, and ALK (Figure 1D). The positivity of focal cytokeratin, which has been reported in a small proportion of ALK+LBCL cases,¹⁵ and the cytomorphology of this case may have led to a misdiagnosis of undifferentiated metastatic carcinoma. The presence of *ALK* translocation was demonstrated by an ALK split FISH assay, which was performed at a commercial laboratory (*data not shown*). The tumor cells were positive for PAX5, which is suggestive of ALK+LBCL. However, we carefully excluded a possibility of metastasis of ALK-positive lung cancer¹⁰ because the tumor cells were positive for some cytokeratins and immunohistochemistry for immunoglobulins was not evaluable due to background staining. Immunohistochemistry for TTF1 was negative; this is usually positive in ALK-positive lung cancers.¹⁶ In addition, PCR and sequencing analyses revealed that *IGH* was monoclonally rearranged and somatically hypermutated (*data not shown*).

The patient was diagnosed as having ALK+LBCL and achieved complete remission after 6 cycles of cyclophosphamide, doxorubicin, vincristine, and prednisone (CHOP) treatment. Four months later, however, he relapsed.

Identification of *SQSTM1*-ALK

The 2 major ALK fusions in ALK+LBCL are CLTC-ALK and NPM-ALK, and they show a coarse granular cytoplasmic pattern and a nuclear and cytoplasmic pattern in anti-ALK immunohistochemistry, respectively. In the present case, anti-ALK immunohistochemistry showed a diffuse cytoplasmic staining pattern with ill-demarcated spots (Figure 1D), which was different from either of the former 2 patterns. Therefore, we carried out inverse RT-PCR to examine the presence of a novel fusion of *ALK*. We indeed isolated a cDNA containing the exon 5 of *SQSTM1* in-frame fused to the exon 20 of *ALK* (Figure 2A). A separate RT-PCR assay amplified the fusion point of *SQSTM1*-ALK cDNA (*data not shown*). To confirm the chromosome rearrangement, we performed *SQSTM1*-ALK fusion FISH. This result was consistent with the presence of a t(2;5)(p23.1;q35.3) leading to the generation of *SQSTM1*-ALK (Figure 2B). The complete sequences of *SQSTM1*-ALK are shown in the *Online Supplementary Figure S1*.

SQSTM1 is an ubiquitin binding protein that is associated with oxidative stress, cell signaling, and autophagy.¹⁷⁻²⁰ Autophagosomal membrane protein LC3/Atg8 binds *SQSTM1* and makes *SQSTM1*-containing protein aggregate to the autophagosome.²¹ Mutations within *SQSTM1* are identified in patients with Paget's disease of bone.²²

SQSTM1 is located very near *NPM*, which is on 5q35.1. Therefore, the cytogenetic findings of the NPM-ALK-positive and the *SQSTM1*-ALK-positive lymphomas may be similar, and this may mean that *SQSTM1*-ALK occurrence in lymphoma may be underestimated. As mentioned, however, NPM-ALK and *SQSTM1*-ALK differ in terms of the anti-ALK immunostaining pattern. NPM has a nuclear transport signal, while *SQSTM1* does not. Therefore, NPM-ALK shows a nuclear and cytoplasmic staining pattern while *SQSTM1*-ALK shows only a cytoplasmic staining pattern. ALK is a representative "promiscuous" molecule because of its various fusion partners. The subcellular localization of ALK fusions depends on the fusion partners. The anti-ALK immunohistochemical staining pattern is, therefore, a simple and useful means to identify the possible partner in a tested case and, in fact, has prompt-

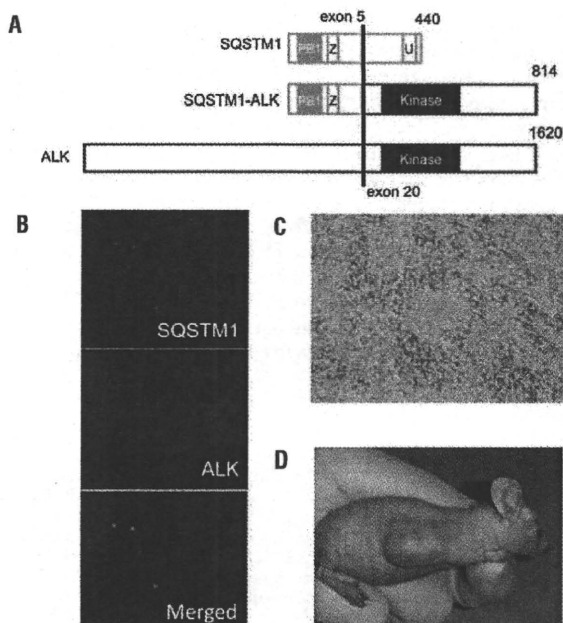


Figure 2. Discovery of *SQSTM1*-ALK fusion gene. (A) A chromosome translocation, t(2;5)(p23.1;q35.3), generates a cDNA fusion in which exon 5 of *SQSTM1* is joined to the *ALK* cDNA for the intracellular region of its encoded protein (containing the tyrosine kinase domain). Numbers indicate amino acid positions of each protein. PB1: Phox and Bem1p; Z: atypical zinc finger; U: ubiquitin-associated. (B) A section of the specimen for the present case was subjected to FISH with an *SQSTM1*-ALK fusion assay. Nuclei are stained blue with DAPI. (C) Murine 3T3 fibroblasts were infected with retroviruses expressing *SQSTM1*-ALK. The cells were photographed after culture for 14 days. (D) A nude mouse was injected subcutaneously with 3T3 cells infected as in (C), and tumor formation was examined after 20 days.

ed the identification of many ALK fusion partners, including the present case.

Transforming activities of *SQSTM1*-ALK

We generated a recombinant retrovirus encoding *SQSTM1*-ALK and used it to infect cultured 3T3 fibroblasts. Infection with the virus, but not with an empty virus, resulted in the formation of multiple transformed foci *in vitro* (Figure 2C). As control experiments for formation, EML4-ALK (variant 1) and NPM-ALK similarly produced transformed foci (*data not shown*). The same 3T3 cells were injected into nude mice for an *in vivo* tumorigenicity assay. As expected, 3T3 cells expressing *SQSTM1*-ALK developed subcutaneous tumors at all injection sites within an observation period of 20 days (Figure 2D), confirming the transforming potential of the novel fusion kinase, *SQSTM1*-ALK.

All ALK fusion partners identified so far except moesin (MSN) have a coiled-coil domain(s) in their sequences, and the domain is conserved in its fusion form. The coiled-coil domain allows the protein to homodimerize. The tyrosine kinase domain of the ALK fusions is constitutively phosphorylated and activated through homodimerization via

the coiled-coil domain. It has been speculated that the binding properties of MSN to cell membrane proteins lead to the dimerization of MSN-ALK proteins, enabling the constitutive phosphorylation of the chimeric MSN-ALK protein.²³ SQSTM1 does not harbor a coiled-coil domain and does not bind to membrane proteins. Instead, it has the Phox and Bem1p (PB1) domain in its N-terminus and forms heteromeric and homomeric complexes mediated by this domain.²⁴ Therefore, SQSTM1-ALK probably homodimerizes through the PB1 domain, leading to constitutive activation of the ALK kinase domain.

In conclusion, we reported a novel ALK fusion, SQSTM1-ALK, and its oncogenicity. ALK+LBCL is an aggressive lymphoma with poor prognosis;³ ALK

inhibitors are promising therapeutic agents for this condition. SQSTM1-ALK may be a rare fusion, but our data provide novel biological insights and may serve as a key to the accurate diagnosis of this rare lymphoma.

Authorship and Disclosures

The information provided by the authors about contributions from persons listed as authors and in acknowledgments is available with the full text of this paper at www.haematologica.org.

Financial and other disclosures provided by the authors using the ICMJE (www.icmje.org) Uniform Format for Disclosure of Competing Interests are also available at www.haematologica.org.

References

- Delsol G, Lamant L, Mariame B, Pulford K, Dastugue N, Brousset P, et al. A new subtype of large B-cell lymphoma expressing the ALK kinase and lacking the 2;5 translocation. *Blood*. 1997;89(5):1483-90.
- Beltran B, Castillo J, Salas R, Quinones P, Morales D, Hurtado F, et al. ALK-positive diffuse large B-cell lymphoma: report of four cases and review of the literature. *J Hematol Oncol*. 2009;2:11.
- Laurent C, Do C, Gascoyne RD, Lamant L, Ysebaert L, Laurent G, et al. Anaplastic lymphoma kinase-positive diffuse large B-cell lymphoma: a rare clinicopathologic entity with poor prognosis. *J Clin Oncol*. 2009;27(25):4211-6.
- Gascoyne RD, Lamant L, Martin-Subero JI, Lestou VS, Harris NL, Muller-Hermelink HK, et al. ALK-positive diffuse large B-cell lymphoma is associated with Clathrin-ALK rearrangements: report of 6 cases. *Blood*. 2003;102(7):2568-73.
- De Paepe P, Baens M, van Krieken H, Verhasselt B, Stul M, Simons A, et al. ALK activation by the CLTC-ALK fusion is a recurrent event in large B-cell lymphoma. *Blood*. 2003;102(7):2638-41.
- Chikatsu N, Kojima H, Suzukawa K, Shinagawa A, Nagasawa T, Ozawa H, et al. ALK+, CD30-, CD20- large B-cell lymphoma containing anaplastic lymphoma kinase (ALK) fused to clathrin heavy chain gene (CLTC). *Mod Pathol*. 2003;16(8):828-32.
- Onciu M, Behm FG, Downing JR, Shurtleff SA, Raimondi SC, Ma Z, et al. ALK-positive plasmablastic B-cell lymphoma with expression of the NPM-ALK fusion transcript: report of 2 cases. *Blood*. 2003;102(7):2642-4.
- Adam P, Katzenberger T, Seeberger H, Gattenlohner S, Wolf J, Steinlein C, et al. A case of a diffuse large B-cell lymphoma of plasmablastic type associated with the t(2;5)(p23;q35) chromosome translocation. *Am J Surg Pathol*. 2003;27(11):1473-6.
- Van Roosbroeck K, Cools J, Dierickx D, Thomas J, Vandenberghe P, Stul M, et al. ALK-positive large B-cell lymphomas with cryptic SEC31A-ALK and NPM1-ALK fusions. *Haematologica*. 2010;95(3):509-13.
- Takeuchi K, Choi YL, Togashi Y, Soda M, Hatano S, Inamura K, et al. KIF5B-ALK, a novel fusion oncokine identified by an immunohistochemistry-based diagnostic system for ALK-positive lung cancer. *Clin Cancer Res*. 2009;15(9):3143-9.
- Soda M, Choi YL, Enomoto M, Takada S, Yamashita Y, Ishikawa S, et al. Identification of the transforming EML4-ALK fusion gene in non-small-cell lung cancer. *Nature*. 2007;448(7153):561-6.
- Takeuchi K, Choi YL, Soda M, Inamura K, Togashi Y, Hatano S, et al. Multiplex reverse transcription-PCR screening for EML4-ALK fusion transcripts. *Clin Cancer Res*. 2008;14(20):6618-24.
- Choi YL, Takeuchi K, Soda M, Inamura K, Togashi Y, Hatano S, et al. Identification of novel isoforms of the EML4-ALK transforming gene in non-small cell lung cancer. *Cancer Res*. 2008;68(13):4971-6.
- Onishi M, Kinoshita S, Morikawa Y, Shibuya A, Phillips J, Lanier LL, et al. Applications of retrovirus-mediated expression cloning. *Exp Hematol*. 1996;24:324-9.
- Reichard KK, McKenna RW, Kroft SH. ALK-positive diffuse large B-cell lymphoma: report of four cases and review of the literature. *Mod Pathol*. 2007;20(3):310-9.
- Inamura K, Takeuchi K, Togashi Y, Hatano S, Ninomiya H, Motoi N, et al. EML4-ALK lung cancers are characterized by rare other mutations, a TTF-1 cell lineage, an acinar histology, and young onset. *Mod Pathol*. 2009;22(4):508-15.
- Komatsu M, Kurokawa H, Waguri S, Taguchi K, Kobayashi A, Ichimura Y, et al. The selective autophagy substrate p62 activates the stress responsive transcription factor Nrf2 through inactivation of Keap1. *Nat Cell Biol*. 2010;12(3):213-23.
- Kirkin V, McEwan DG, Novak I, Dikic I. A role for ubiquitin in selective autophagy. *Mol Cell*. 2009;34(3):259-69.
- Seibenhener ML, Geetha T, Wooten MW. Sequestosome 1/p62--more than just a scaffold. *FEBS Lett*. 2007;581(2):175-9.
- Bjorkoy G, Lamark T, Johansen T. p62/SQSTM1: a missing link between protein aggregates and the autophagy machinery. *Autophagy*. 2006;2(2):138-9.
- Pankiv S, Clausen TH, Lamark T, Brech A, Bruun JA, Outzen H, et al. p62/SQSTM1 binds directly to Atg8/LC3 to facilitate degradation of ubiquitinated protein aggregates by autophagy. *J Biol Chem*. 2007;282(33):24131-45.
- Laurin N, Brown JE, Morissette J, Raymond V. Recurrent mutation of the gene encoding sequestosome 1 (SQSTM1/p62) in Paget disease of bone. *Am J Hum Genet*. 2002;70(6):1582-8.
- Tort F, Pinyol M, Pulford K, Roncador G, Hernandez L, Nayach I, et al. Molecular characterization of a new ALK translocation involving moesin (MSN-ALK) in anaplastic large cell lymphoma. *Lab Invest*. 2001;81(3):419-26.
- Lamark T, Perander M, Outzen H, Kristiansen K, Overvatn A, Michaelsen E, et al. Interaction codes within the family of mammalian Phox and Bem1p domain-containing proteins. *J Biol Chem*. 2003;278(36):34568-81.



Early Release Paper

Overexpression of enhancer of zeste homolog 2 with trimethylation of lysine 27 on histone H3 in adult T-cell leukemia/lymphoma as a target for epigenetic therapy

by Daisuke Sasaki, Yoshitaka Imaizumi, Hiroo Hasegawa, Akemi Osaka, Kunihiro Tsukasaki, Young Lim Choi, Hiroyuki Mano, Victor Marquez, Tomayoshi Hayashi, Katsunori Yanagihara, Yuji Moriwaki, Yasushi Miyazaki, Shimeru Kamihira, and Yasuaki Yamada

Haematologica 2010 [Epub ahead of print]

Citation: Sasaki D, Imaizumi Y, Hasegawa H, Osaka A, Tsukasaki K, Choi YL, Mano H, Marquez V, Hayashi T, Yanagihara K, Moriwaki Y, Miyazaki Y, Kamihira S, and Yamada Y. Overexpression of enhancer of zeste homolog 2 with trimethylation of lysine 27 on histone H3 in adult T-cell leukemia/lymphoma as a target for epigenetic therapy. *Haematologica*. 2010; 95:xxx
doi:10.3324/haematol.2010.028605

Publisher's Disclaimer.

E-publishing ahead of print is increasingly important for the rapid dissemination of science. Haematologica is, therefore, E-publishing PDF files of an early version of manuscripts that have completed a regular peer review and have been accepted for publication. E-publishing of this PDF file has been approved by the authors. After having E-published Ahead of Print, manuscripts will then undergo technical and English editing, typesetting, proof correction and be presented for the authors' final approval; the final version of the manuscript will then appear in print on a regular issue of the journal. All legal disclaimers that apply to the journal also pertain to this production process.

Haematologica (pISSN: 0390-6078, eISSN: 1592-8721, NLM ID: 0417435, www.haematologica.org) publishes peer-reviewed papers across all areas of experimental and clinical hematology. The journal is owned by the Ferrata Storti Foundation, a non-profit organization, and serves the scientific community with strict adherence to the principles of open access publishing (www.doaj.org). In addition, the journal makes every paper published immediately available in PubMed Central (PMC), the US National Institutes of Health (NIH) free digital archive of biomedical and life sciences journal literature.

Support Haematologica and Open Access Publishing by becoming a member of the European Hematology Association (EHA) and enjoying the benefits of this membership, which include free participation in the online CME program

Overexpression of enhancer of zeste homolog 2 with trimethylation of lysine 27 on histone H3 in adult T-cell leukemia/lymphoma as a target for epigenetic therapy

Daisuke Sasaki,¹ Yoshitaka Imaizumi,² Hiroo Hasegawa,¹ Akemi Osaka,¹ Kunihiro Tsukasaki,² Young Lim Choi,³ Hiroyuki Mano,³ Victor E. Marquez,⁴ Tomayoshi Hayashi,⁵ Katsunori Yanagihara,¹ Yuji Moriwaki,² Yasushi Miyazaki,² Shimeru Kamihira,¹ and Yasuaki Yamada¹

¹Department of Laboratory Medicine, Nagasaki University Graduate School of Biomedical Sciences, Nagasaki, Japan; ²Department of Hematology and Molecular Medicine, Atomic Bomb Disease Institute, Nagasaki University Graduate School of Biomedical Sciences, Nagasaki, Japan; ³Division of Functional Genomics, Jichi Medical University, Tochigi, Japan; ⁴Chemical Biology Laboratory, National Cancer Institute, Frederick, MD, USA, and ⁵Department of Pathology, Nagasaki University Hospital, Nagasaki, Japan

Funding

supported in part by a Grant-in-Aid for Scientific Research from the Ministry of Health, Labour, and Welfare of Japan (No. 04010119). For VEM, this research was supported in part by the Intramural Research Program of the NIH, Center for Cancer Research, NCI-Frederick.

Acknowledgments

The authors thank Sayaka Mori and Yuko Doi for excellent technical assistance.

Correspondence

Yasuaki Yamada, Department of Laboratory Medicine, 1-7-1 Sakamoto, Nagasaki 852-8501, Japan. Phone: international +81.2958197408.

Fax: international +81.959197422. E-mail: y-yamada@nagasaki-u.ac.jp

ABSTRACT

Background

Enhancer of zeste homolog 2 is a component of the Polycomb repressive complex 2 that mediates chromatin-based gene silencing through trimethylation of lysine 27 on histone H3. This complex plays vital roles in the regulation of development-specific gene expression.

Design and Methods

In this study, a comparative microarray analysis of gene expression in primary adult T-cell leukemia/lymphoma samples was performed, and the results were evaluated for their oncogenic and clinical significance.

Results

Significantly higher levels of *Enhancer of zeste homolog 2* and *RING1* and *YY1 binding protein* transcripts with enhanced levels of trimethylation of lysine 27 on histone H3 were found in adult T-cell leukemia/lymphoma cells compared with those in normal CD4⁺ T-cells. Furthermore, there was an inverse correlation between the expression level of *Enhancer of zeste homolog 2* and that of miR-101 or miR-128a, suggesting that the altered expression of the latter miRNAs accounts for the overexpression of the former. Patients with high *Enhancer of zeste homolog 2* or *RING1* and *YY1 binding protein* transcripts had a significantly worse prognosis than those without it, indicating a possible role

of these genes in the oncogenesis and progression of this disease. Indeed, adult T-cell leukemia/lymphoma cells were sensitive to a histone methylation inhibitor, 3-deazaneplanocin A. Furthermore, 3-deazaneplanocin A and histone deacetylase inhibitor panobinostat showed a synergistic effect in killing the cells.

Conclusions

These findings reveal that adult T-cell leukemia/lymphoma cells have deregulated Polycomb repressive complex 2 with overexpressed Enhancer of zeste homolog 2, and that there is the possibility of a new therapeutic strategy targeting histone methylation in this disease.

Introduction

The Polycomb group (PcG) proteins play critical roles in the regulation of development by repressing specific sets of developmental genes through chromatin modification.¹ They form two distinct multimeric complexes, Polycomb repressive complex 1 (PRC1) and PRC2, which bind to polycomb responsive elements (PRE), repress genes required for cell differentiation, and maintain pluripotency and self-renewal of embryonic stem cells and hematopoietic stem cells.^{2,3} PRC2 consists of Enhancer of zeste homolog 2 (EZH2), which has histone methyltransferase activity, suppressor of zeste 12 (SUZ12), and embryonic ectoderm development (EED), which is required to maintain the integrity of PRC2.^{1,4} Sequence-specific DNA binding protein YY1,

which recognizes PRE, interacts with EED and recruits PRC2 to a specific chromatin domain to be repressed.⁵ EED interacts with histone deacetylase (HDAC) proteins, HDAC1 and HDAC2, and the histone binding proteins RBBP4 (RbAp48) and RBBP7 (RbAp46).⁶ PRC2 thus also participates in histone deacetylation. EZH2, as a part of the PRC2 complex, not only methylates histone but also serves as a recruitment platform for DNA methyltransferases that methylate the promoter regions of target genes, which is another mechanism of gene repression.⁷ The more diverse complex PRC1 consists of HPC family proteins that mediate chromatin association, HPH family proteins, RING, BMI1, and others.¹ PRC2 initiates trimethylation of lysine 27 on histone H3 (H3K27me3) and, to a lesser extent, lysine 9 of histone H3.⁸ PRC1 recognizes H3K27me3 through the chromodomain of the HPC and maintains the trimethylation. There are a number of reports indicating that such epigenetically mediated transcriptional silencing is associated with cancer development.^{1,9} Among these, oncogenic roles of overexpressed EZH2 have been studied in a variety of tumors.¹⁰

Adult T-cell leukemia/lymphoma (ATL) is a neoplasm of mature CD4+ T-cell origin, etiologically associated with human T-cell leukemia virus type-1 (HTLV-1).^{11,12} Its clinical behavior is quite diverse among patients and is subclassified into four subtypes, smoldering type and chronic type as indolent subtypes, and acute type and lymphoma type as aggressive subtypes.¹³ Inactivation of tumor suppressor genes is one of the key events in development and progression, and there is a strong accumulation of *p14ARF/p15INK4B/p16INK4A* gene deletion/methylation or *p53* gene mutations in aggressive subtypes (>60%).¹⁴⁻²⁰ In the present study, for further

investigation of the oncogenesis of ATL, we performed a comparative microarray analysis of gene expression in primary ATL samples. ATL cells expressed significantly higher levels of *EZH2* and *RYBP* (RING1 and YY1 binding protein) transcripts than CD4⁺ T cells from healthy volunteers. Moreover, acute-type ATL cells showed significantly higher levels of these transcripts than chronic-type ATL cells, suggesting that deregulation of PcG proteins plays a crucial role not only in the development but also in the progression of ATL. In addition, ATL samples were strongly positive for H3K27me3, and were sensitive to 3-deazaneplanocin A (DZNep), a histone methylation inhibitor.²¹⁻²³ It has recently been shown that HDAC inhibitor panobinostat (PS, also known as LBH589) depletes the levels of EZH2, SUZ12, and EED and induces apoptotic death in leukemia cells.²⁴ Deregulation of PcG protein genes with overexpressed EZH2 in ATL cells suggests that ATL is one of the appropriate target diseases for such epigenetic therapy.

Design and Methods

Sample preparation

This study was approved by the ethics committees of Nagasaki University, and all clinical samples were obtained after written informed consent was provided. The diagnosis of ATL was confirmed by the monoclonal integration of HTLV-1 proviral DNA in the genomic DNA of leukemia cells. Peripheral blood mononuclear cells (PBMCs) were obtained from ATL patients (acute type 22 cases, chronic type 19 cases) and healthy adult volunteers by density gradient

centrifugation using Lympho-prep (AXIS SHIELD, Oslo, Norway). For enrichment of ATL cells, CD4⁺ cells were purified from the PBMCs by the magnetic bead method (CD4 MicroBeads, Miltenyi Biotec, Auburn, CA) as described elsewhere.²⁵ Besides these samples for microarray analysis, we prepared another set of samples for quantitative real-time RT-PCR (qRT-PCR) and western blotting (25 ATL patients, 13 HTLV-1 carriers, and 12 healthy adults), to confirm the results of microarray analysis. We also used formalin-fixed, paraffin-embedded lymph nodes from 7 patients with lymphoma-type ATL and 5 patients with follicular lymphoma for immunohistochemical analysis.

ATL cell lines used in this study, SO4, ST1, KK1, KOB, and LM-Y1, were established from respective patients in our laboratory and have been confirmed to be of primary ATLL cell origin.²⁶ Cells were maintained in RPMI1640 medium supplemented with 10% FBS and 100 Japan reference units of recombinant interleukin-2 (rIL-2) (kindly provided by Takeda Pharmaceutical Company, Ltd., Osaka, Japan). We also used HTLV-1-infected T-cell lines MT2 and HuT102 and acute T-lymphoblastic leukemia cell lines Jurkat and MOLT4, which were maintained without rIL-2.

DNA microarray analysis

RNA was prepared from purified CD4⁺ T cells, and subjected to hybridization to HGU133A & B microarray containing 44,760 probe sets for human genes (Affymetrix, Santa Clara, CA, USA) as described previously.^{25,27} The mean expression intensity of the internal positive control probe sets (http://www.affymetrix.com/support/technical/mask_files.affx) was set to 500

units in each hybridization, and the fluorescence intensity of each test gene was normalized accordingly. All HGU133A & B microarray data are available at the Gene Expression Omnibus website (<http://www.ncbi.nlm.nih.gov/geo>) under the accession number GSE1466.

Quantitative real-time RT-PCR

For confirmation of the results of microarray analysis, we performed quantitative real-time RT-PCR (qRT-PCR) for PcG protein genes. Total RNA was prepared using Isogen (Wako, Osaka, Japan). After removal of contaminated DNA with DNase (Message Clean kit; GenHunter, Nashville, TN), cDNA was constructed from 1 µg of total RNA using the SuperScript III RT-PCR System (Invitrogen, Carlsbad, CA, USA) according to the manufacturer's instructions. Primers and TaqMan probes labeled with TAMRA dye at the 3' end and FAM at the 5' end are listed in Table 1. The mRNA levels for PcG family proteins and porphobilinogen deaminase (PBGD) were measured from a cDNA template using a LightCycler480 PCR System (Roche Diagnostics, Mannheim, Germany). Briefly, reactions were performed in a 20 µl volume with 5 µl (5 ng) of cDNA, 0.5 µM PCR primers, 0.1 µM TaqMan probes, and 10 µl of LightCycler 480 probes Master Mix (Roche Diagnostics). The PCR program consisted of 95°C for 5 min followed by 50 cycles of 95°C for 10 sec and 60°C for 30 sec. After 50 cycles, the absolute amounts of PcG protein mRNA and *PBGD* mRNA were interpolated from the standard curves generated by the dilution method using plasmids derived from a clone transfected with pTAC-1 Vector (BioDynamics Laboratory Inc., Tokyo, Japan) containing amplicons from the PcG family protein and *PBGD* genes, respectively. To normalize these results

for variability in concentration and integrity of RNA and cDNA, the *PBGD* gene was used as an internal control in each sample.

For the quantitative PCR for microRNAs (miRNAs), miR-101, miR-26a, and miR-128a, 10 ng of total RNA (containing miRNA) was used. RT reaction and real-time quantification were performed using TaqMan MicroRNA RT kit and TaqMan MicroRNA assays (hsa-miR-26a, assay ID 000405; hsa-miR-101, assay ID 002253; hsa-miR-128a, assay ID 002216; RNU6B, assay ID 001093) (Applied Biosystems, Foster City, CA, USA) in accordance with the manufacturer's instructions. Each PCR reaction mixture contained 10 μ l of LightCycler 480 probes Master Mix, 4 μ l of nuclease-free water, 1 μ l of 20X specific PCR primer, and 5 μ l of RT product. Thermal cycler was programmed as follows: 95°C for 5 minutes, 40 cycles of 95°C for 15 sec, and 60°C for 60 sec. Using the comparative CT method, we used an endogenous control (RNU6B) to normalize the expression levels of target micro-RNA by correcting differences in the amount of RNA loaded into qPCR reactions.

Western blot analysis and antibodies

Western blot analysis was performed as described previously.²⁸ The analysis was performed using antibodies to EZH2 and Histone H3 (Cell Signaling Technology, Danvers, MA, USA), phospho EZH2 (Ser21) (Bethyl Laboratories, Montgomery, TX), H3K27me3, dimethylated H3K27 (H3K27me2), monomethylated H3K27 (H3K27me1) (Millipore, Temecula, CA, USA), and β -actin (Sigma, St. Louis, MO, USA).

Immunohistochemistry

Immunohistochemical staining for EZH2 and H3K27me3 was performed on formalin-fixed, paraffin-embedded lymph node samples from lymphoma-type ATL patients and follicular lymphoma patients as a control. The deparaffinized slides were pretreated with DAKO Target Retrieval Solution, pH 9 (DAKO Japan, Tokyo, Japan), and heated in a water bath at 95°C for 40 minutes. For all stains, the endogenous peroxidase was quenched using 3% H₂O₂ for 15 minutes. Sections were then placed in 0.5% non-fat dry milk for 30 minutes at room temperature. The primary antibodies used were anti-EZH2 antibody (BD Biosciences, San Jose, CA, USA) and anti-H3K27me3 antibody (Cell Signaling Technology, Boston, MA, USA), and were applied at 1:50 dilution and 1:100 dilution, respectively. They were allowed to react for 1 hour at room temperature, and then the DAKO EnVision™ + Dual Link System-HRP (DAKO Japan, Tokyo, Japan) was applied using diaminobenzidine as the chromogen, following the manufacturer's protocol.

Sensitivity of adult T-cell leukemia/lymphoma cell lines to DZNep and PS (LBH589)

DZNep was synthesized by one of the authors, V.E.M. Cells were treated with different concentrations of DZNep for 72 hours and the cell proliferation status was evaluated by a MTS assay using a Cell Titer 96® AQueos Cell Proliferation Assay kit (Promega, Madison, WI, USA) in accordance with the manufacturer's instructions. To analyze the synergistic effect of combined treatment with DZNep and PS (LBH589) (kindly provided by Novartis Pharma AG, Basel, Switzerland), cells were treated with DZNep (0.3-5.0 µM) and PS

(LBH589) (3-50 nM) for 48 hours. After the cell proliferation status was evaluated by a MTS assay, the combination index (CI) for each drug combination was obtained by determining the median dose effect of Chou and Talalay using the CI equation within the commercially available software CalcuSyn (Biosoft).²⁹ $CI < 1$, $CI = 1$, and $CI > 1$ indicate synergism, additive effect, and antagonism, respectively. Cell viability represents the value relative to that of the control culture without these agents.

Results

Microarray analysis shows increased EZH2 and/or RYBP transcripts in adult T-cell leukemia/lymphoma cells

In a comparative microarray analysis of primary ATL samples, we focused on investigating PcG protein genes, *EZH2*, *RYBP*, *BMI-1*, and *CBX7*, in the present study because ATL cells show many aberrantly hypermethylated DNA sequences.³⁰ ATL cells expressed significantly higher levels of *EZH2* and *RYBP* transcripts than CD4⁺ T-cells from healthy adults (Figure 1A, B). In addition, there was a difference between ATL subtypes in these expressions, and cells from the acute type showed significantly higher levels of these transcripts than the cells from the chronic type. When patients were separated into two groups consisting of those with high expression and those with low expression, the group with high *EZH2* or high *RYBP* transcript showed significantly shorter survival than the respective low-expression groups (Figure 1E, F), indicating that high *EZH2* and/or *RYBP* expression is associated with

aggressive clinical behavior. Convincingly, there was a trend toward accumulation of acute-type ATL in high *EZH2* or high *RYBP* expression group: 14 cases of acute type and 6 cases of chronic type in high *EZH2* group, 7 cases of acute type and 13 cases of chronic type in low *EZH2* group, 14 cases of acute type and 6 cases of chronic type in high *RYBP* group, and 7 cases of acute type and 13 cases of chronic type in low *RYBP* group. BMI1 is known to downregulate the expression of *p14ARF/p16INK4A* and lead to neoplastic transformation.³¹ Chromobox 7 (*CBX7*), a component of the PRC1, is also known to repress the transcription of *p14ARF/p16INK4A*.³² Since inactivation of *p14ARF/p15INK4B/p16INK4A* genes is one of the key events in ATL progression, expression of *BMI-1* and/or *CBX7* transcript was expected to be elevated in acute-type ATL cells. There was however no difference in these expressions between ATL subtypes or even between ATL cells and normal CD4+ T-cells (Figure 1C, D). There was no difference in survival for different *BMI-1* or *CBX7* expression levels (Figure 1G, H).

Confirmation of increased EZH2 and/or RYBP transcripts by quantitative real-time RT-PCR

For confirmation of the results of microarray analysis, we quantified the transcripts of the PcG protein genes including *EZH2* and *RYBP* by qRT-PCR using another set of samples from ATL patients, healthy adults, HTLV-1 carriers, and hematologic cell lines including ATL cell lines. In accordance with the results of microarray analysis, *EZH2* and *RYBP* transcripts were increased in primary ATL cells compared with those in the cells from healthy adults and HTLV-1 carriers, with statistically significantly higher values in *EZH2* in terms of

both absolute copy number per 25 ng of total RNA and normalized expression level (Figure 2A, a, B, b). *RBBP4* was significantly higher in primary ATL cells than in the cells from healthy adults and HTLV-1 carriers in terms of normalized expression level (Figure 2C, c). In contrast, there was no difference in *BMI1*, *YY1*, and *EED* expressions among these groups, although some patients showed very high *BMI1* expression (Figure 2D, d, E, e, F, f). Similarly to primary ATL cells, some ATL cell lines showed high *EZH2* expression in terms of absolute copy number per 25 ng of total RNA (Figure 2A).

EZH2 protein expression with trimethylation of H3K27 is characteristic in adult T-cell leukemia/lymphoma cells

We then examined EZH2 and RYBP at the protein level by western blotting. A 98-kDa band for EZH2 protein and a 32-kDa band for RYBP protein were detected in all primary ATL samples irrespective of subtype, but they were hardly detected in cells from healthy adults and HTLV-1 carriers (Figure 3A, Supplementary Figure 1, and data not shown). ATL cell lines and acute T-lymphoblastic leukemia cell lines also showed intense EZH2 bands. The serine-threonine kinase Akt phosphorylates EZH2 at serine 21 and suppresses its methyltransferase activity by impeding EZH2 binding to histone H3, which results in a decrease in lysine 27 trimethylation.³³ EZH2 of ATL cells was not phosphorylated and was in its active form (Figure 3A). In fact, most primary ATL samples showed the band for H3K27me3, while the cells from healthy adults lacked the band (Figure 3B). As it is known that EZH2 plays a crucial role in trimethylation but not in dimethylation or monomethylation, the bands for H3K27me2 and H3K27me1 were detected in all samples examined, but the

band for H3K27me3 was limited in primary ATL cells and ATL cell lines LMY1 and KOB that showed an intense EZH2 band with a faint phosphorylated EZH2 band (Figure 3A, B). In contrast, EZH2 was strongly phosphorylated in ATL cell lines ST1, SO4, KK1, and acute T-lymphoblastic leukemia cell lines Jurkat and MOLT4, and these cell lines hardly showed the band for H3K27me3. Collectively, these results indicate that ATL cells express functionally active EZH2, and as a result, their H3K27 are trimethylated, and that ATL cell lines LMY1 and KOB preserve such character of primary ATL cells.

Immunohistochemical confirmation of the expression of EZH2 and H3K27me3 in lymph nodes

We next used lymph nodes from lymphoma-type ATL patients for immunohistochemical evaluation of EZH2 expression and H3K27me3. In agreement with the results of western blotting, all ATL lymph nodes from 7 patients were strongly positive for both EZH2 and H3K27me3 without exception in their nuclear staining (Figure 4 and data not shown), suggesting that overexpression of EZH2 with H3K27me3 is a common feature of ATL cells irrespective of ATL subtypes. In contrast, in lymph nodes from 5 follicular lymphoma patients, only a few cells were positive for EZH2 with some variation among patients and most cells were negative for H3K27me3 (Figure 4 and *data not shown*).